EBioMedicine 36 (2018) 140–150

Contents lists available at ScienceDirect

EBioMedicine

journal homepage: www.ebiomedicine.com

EBioMedicine
Published by THE LANCET

Research paper

AMSC-derived exosomes alleviate lipopolysaccharide/D-galactosamine-induced acute liver failure by miR-17-mediated reduction of TXNIP/NLRP3 inflammasome activation in macrophages

Yanning Liu [a,*], Guohua Lou [a], Aichun Li [a], Tianbao Zhang [a], Jinjin Qi [a], Dan Ye [b], Min Zheng [a,*], Zhi Chen [a]

[a] State Key Laboratory for Diagnosis and Treatment of Infectious Diseases, Collaborative Innovation Center for Diagnosis and Treatment of Infectious Diseases, The First Affiliated Hospital of School of Medicine, Zhejiang University, Hangzhou, China.
[b] Department of Endocrinology and Metabolism, The First Affiliated Hospital of School of Medicine, Zhejiang University, Hangzhou, China.

ARTICLE INFO

Article history:
Received 29 May 2018
Received in revised form 28 August 2018
Accepted 28 August 2018
Available online 6 September 2018

Keywords:
Mesenchymal stem cells
Exosome
Macrophage
miR-17
TXNIP
NLRP3 inflammasome

ABSTRACT

Background: Mesenchymal stem cell (MSC)-derived exosome administration has been considered as a novel cell-free therapy for liver diseases through cell-cell communication. This study was aimed to determine the effects and mechanisms of AMSC-derived exosomes (AMSC-Exo) for acute liver failure (ALF) treatment.
Methods: AMSC-Exo were intravenously administrated into the mice immediately after lipopolysaccharide and D-galactosamine (LPS/GalN)-exposure and their effects were evaluated by liver histological and serum biochemical analysis. To elucidate its mechanisms in ALF therapy, the expression levels of miRNAs and inflammasome-related genes in macrophages were evaluated by qPCR and Western blot analysis, respectively. The exosomes from miR-17-knockdowned AMSCs (AMSC-Exo$^{miR\text{-}17\text{-}KD}$) were used for further determine the role of miR-17 in AMSC-Exo-based therapy.
Findings: AMSC-Exo administration significantly ameliorated ALF as determined by reduced serum alanine aminotransferase and aspartate aminotransferase levels and hepatic inflammasome activation. Further experiments revealed that AMSC-Exo were colocalized with hepatic macrophages and could reduce inflammatory factor secretion by suppressing inflammasome activation in macrophages. Moreover, miR-17, which can suppress NLRP3 inflammasome activation by targeting TXNIP, was abundant in AMSC-Exo cargo. While, the therapeutic effects of AMSC-Exo$^{miR\text{-}17\text{-}KD}$ on ALF were significantly abolished as they could not effectively suppress TXNIP expression and consequent inflammasome activation *in vitro* and *in vivo*.
Interpretation: Exosome-shuttled miR-17 plays an essential role in AMSC-Exo therapy for ALF by targeting TXNIP and suppressing inflammasome activation in hepatic macrophages. AMSC-Exo-based therapy may present as a promising approach for TXNIP/NLRP3 inflammasome-related inflammatory liver diseases.
Fund: Key R&D projects of Zhejiang province (2018C03019) and National Natural Science Fund (81470851 and 81500616).
© 2018 The Authors. Published by Elsevier B.V. This is an open access article under the CC BY-NC-ND license (http://creativecommons.org/licenses/by-nc-nd/4.0/).

1. Introduction

Acute liver failure (ALF) is a clinical manifestation of sudden and severe hepatic injury caused by viruses, drugs, toxins, or alcohol. It leads to hepatic encephalopathy, hepatorenal syndrome, severe infection, and multiple organ failure and is associated with high mortality rate [1]. Orthotopic liver transplantation (OLT) and artificial liver therapies are presented as the two main treatments for ALF in clinical. However, the shortage of available donor livers and multiple postoperative complications limit the widespread clinical application of OLT and the efficacy of artificial liver therapy is relatively limited. Recently, mesenchymal stem cell (MSC) transplantation has emerged as a promising strategy for treating liver diseases including ALF through tissue repair and immune regulation [2]. An increasing number of studies have shown that the mechanism of MSC repaired tissue injury is related to paracrine action rather than direct transdifferentiation. MSC-secreted exosomes may contribute to the therapeutic potency of MSCs by mediating cell-cell micro-communication and transporting paracrine factors during angiogenesis, tissue regeneration, and immune regulation [3,4]. Our previous study showed that exosomes can mediate the therapeutic effect of miR-122-modified adipose tissue-derived MSCs (AMSCs) in liver fibrosis by

* Corresponding authors at: The First Affiliated Hospital, Zhejiang University, 79# Qingchun Road, 6A-17, Hangzhou 310003, China.
E-mail addresses: liuyanning@zju.edu.cn (Y. Liu), louguohua@zju.edu.cn (G. Lou), Liaichun@zju.edu.cn (A. Li), zhangtianbao1994@zju.edu.cn (T. Zhang), yedan_zdyy@zju.edu.cn (D. Ye), minzheng@zju.edu.cn (M. Zheng), zjuchenzhi@zju.edu.cn (Z. Chen).

https://doi.org/10.1016/j.ebiom.2018.08.054
2352-3964/© 2018 The Authors. Published by Elsevier B.V. This is an open access article under the CC BY-NC-ND license (http://creativecommons.org/licenses/by-nc-nd/4.0/).

Research in context

Evidence before this study

Orthotopic liver transplantation (OLT) and artificial liver therapies are presented as the two main treatments for acute liver failure (ALF) in clinical. However, the shortage of available donor livers and multiple postoperative complications limit the widespread clinical application of OLT and the efficacy of artificial liver therapy is relatively limited. Recently, mesenchymal stem cell (MSC) transplantation has emerged as a promising strategy for treating liver diseases including ALF through tissue repair and immune regulation. While, more and more studies have shown that MSC-secreted exosomes may contribute to the therapeutic potency of MSCs by mediating cell-cell micro-communication and transporting paracrine factors during angiogenesis, tissue regeneration, and immune regulation. MSC-derived exosomes have yielded beneficial effects in several experimental models of organ injury. Recently, the therapeutic effects of exosomes from bone marrow-, chorionic plate-, umbilical cord-, or induced pluripotent stem cell-derived MSCs have been reported in a variety of animal models of liver disease, including concanavalin A or acetaminophen-induced acute liver injury, CCl_4-induced liver fibrosis, liver antigen S100-induced autoimmune hepatitis, or I/R-induced hepatic injury. Our previous studies also showed that the exosomes produced by miR-122-modified AMSCs can alleviate liver fibrosis and enhance hepatocellular carcinoma chemosensitivity *via* exosome-mediated miR-122 delivery. Thus, administration of MSC-derived exosomes may represent as an ideal cell-free therapy for liver diseases.
NLRP3 inflammasome activation has been determined in human and experimental ALF and has been identified as a major contributor to hepatocyte damage and immune cell activation and amplification in fulminant hepatitis. Several studies have shown that MSCs can attenuate collagen-induced arthritis, coxsackievirus B3-induced myocarditis, or ischemia/reperfusion (I/R)-induced renal injury by inhibiting NLRP3 inflammasome activation. However, whether AMSC-Exo-based therapy can ameliorate ALF and modulate NLRP3 inflammasome is unclear.

Added value of this study

In this study, we isolated exosomes from adipose tissue-derived MSCs (AMSCs) and found that AMSC-Exo administration could significantly ameliorate LPS/GalN-induced fulminant hepatitis. In addition, AMSC-Exo were found to be colocalized with hepatic macrophages and could reduce inflammatory factor secretion and inflammasome activation in macrophages. Further mechanism study revealed that AMSC-Exo contain high level of miR-17 and suppress NLRP3 inflammasome activation by miR-17-mediated TXNIP inhibition. This study demonstrates that exosome-shuttled miR-17 plays an essential role in AMSC-Exo therapy for ALF by targeting TXNIP and modulating inflammasome activation in hepatic macrophages.

Implications of all the available evidence

This study provides novel insights into MSC-Exo-based therapy and its potential mechanism. Administration of AMSC-Exo may present as a novel therapeutic strategy for preventing fulminant hepatitis, as well as other TXNIP/NLRP3 inflammasome-related inflammatory liver diseases.

delivering miR-122 into hepatic stellate cells, suggesting that the administration of AMSC-derived exosomes (AMSC-Exo) can serve as a novel therapeutic modality for liver disease [5].

The nucleotide-binding and oligomerization domain-like receptor 3 (NLRP3) inflammasome, a newly identified pattern recognition receptor, contains NLRP3, apoptosis-associated speck-like protein (ASC), and procaspase-1 [6]. It is highly expressed in liver and participates in the pathogenesis of various liver diseases [7]. The function of NLRP3 is tightly controlled by the interaction among its three components. The NLRP3 protein recognizes pathogen-associated molecular patterns (PAMPs), danger-associated molecular patterns (DAMPs), other exogenous pathogenic agents, or environmental stresses, which lead to conformational changes in the NLRP3 inflammasome. Subsequently, the adapter protein ASC and procaspase-1 are recruited and bind to the caspase recruitment domain of procaspase, thereby activating caspase-1 by autocatalysis and contributes to the production and secretionof mature interleukin-1 beta (IL-1β) and IL-18 [8]. Further studies showed that deficiency of thioredoxin-interacting protein (TXNIP), which originally acted as a negative regulator of thioredoxin, impairs the activation of the NLRP3 inflammasome and subsequent secretion of IL-1β [9,10]. Moreover, the hepatic expression of TXNIP and the interaction between TXNIP and NLRP3 were up-regulated in an ALF mouse model, suggesting that TXNIP-mediated activation of NLRP3 inflammasome is important for ALF [11]. Therefore, targeting the TXNIP-NLRP3 inflammasome may be an effective strategy for reducing fulminant hepatitis.

Several studies have shown that MSCs can attenuate collagen-induced arthritis, coxsackievirus B3-induced myocarditis, or ischemia/reperfusion (I/R)-induced renal injury by inhibiting NLRP3 inflammasome activation [12–14]. However, whether AMSC-Exo-based therapy can ameliorate ALF and modulate NLRP3 inflammasome is unclear. Lipopolysaccharide and D-galactosamine (LPS/GalN)-induced liver injury is widely used to simulate ALF [15]. The present study aimed to investigate the effects and underlying mechanisms of AMSC-Exo on LPS/GalN-induced ALF.

2. Materials and methods

2.1. Isolation and identification of AMSCs

Mice were purchased from Nanjing BioMedical Research Institute of Nanjing University, and all procedures were reviewed and approved by the Institutional Animal Care and Use Committee of Zhejiang University. Inguinal adipose tissues were obtained from C57BL/6J male mice (8–10 weeks old). Tissues were digested with 0.075% collagenase type I (Sigma), washed with PBS, and then cultured in murine MesenCult™ Expansion Kit (Stemcell) containing 2 mM L-glutamine (Gibco) and 1% antibiotic-antimycotic. Cells were maintained and expanded by 3–6 passages before use. The phenotype profile of AMSCs was evaluated through flow cytometry analysis (BD Accuri® C6 flow cytometer) by using PE-labeled CD29, CD31, CD44, CD45, CD73, CD90.2, CD105, and I-A/I-E (BioLegend) antibodies. PE-labeled IgG1 was used as isotype control. The differentiations of AMSCs to chondrocytes and adipocytes were tested by using StemPro® Chondrogenesis and Cdipogenesis Differentiation Kit (Gibco). Afterward, staining with Oil red O and Alcian Blue was performed to detect adipocytes and chondrocytes, respectively.

2.2. MiRNA inhibitor transfection

The AMSC-conditioned medium consisted of DMEM supplemented with 10% exosome-depleted FBS (VivaCell). Prior to transfection, 1×10^6 AMSCs were seeded in 10 mL of AMSC-conditioned medium overnight. AMSCs were then transfected with 10 nM of miR-17 inhibitor (RiboBio) or 10 nM of miRNA inhibitor negative control (RiboBio) by using Lipofectamine® RNAiMAX (Thermo Fisher). At 48 h after transfection, AMSC supernatant was harvested for exosome isolation.

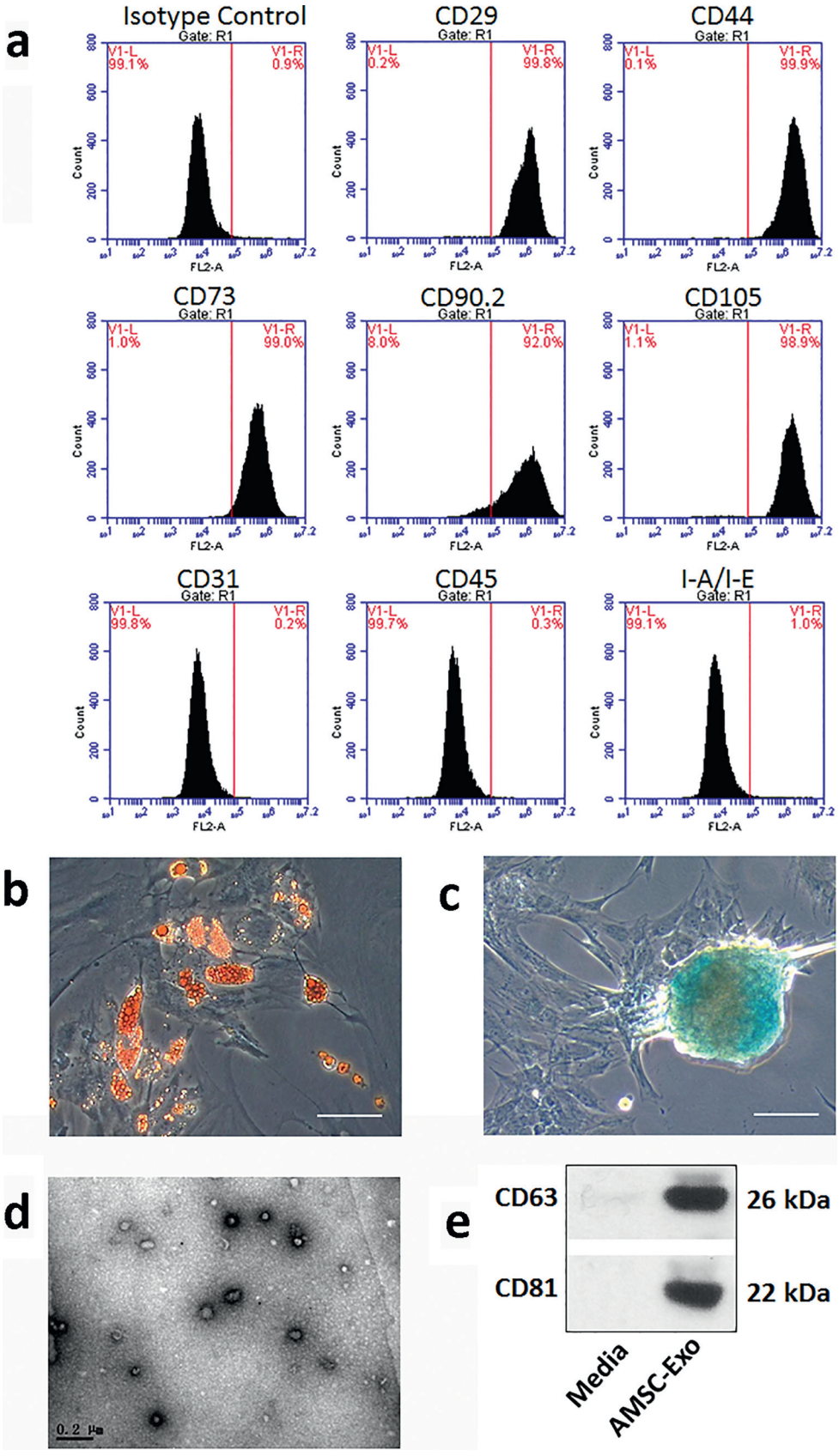

Fig. 1. Characterization of AMSCs and AMSC-Exo. (a) Flow cytometry analysis of AMSC phenotypes. (b) Oil Red O staining of AMSCs cultured in adipogenesis differentiation medium for 14 days. Scale bar: 50 μm. (c) Alcian Blue staining of AMSCs cultured in chondrogenesis differentiation medium for 21 days. Scale bar: 50 μm. (d) Electron microscopy image of AMSC-Exo. (e) Western blot analysis for CD63 and CD81 expression in AMSC-Exo.

2.3. Exosome preparation and harvest

Exosomes were isolated from the AMSC supernatant by using total exosome isolation reagent (Thermo Fisher) in accordance with the manufacturer's instructions. The ultrastructure of exosomes was observed under electron microscopy. Western blot analysis was used to analyze the exosomal surface markers, such as CD63 (1:2000, Abcam) and CD81 (1:2000, Abcam). Precipitates from AMSC supernatant were used as negative control. The protein content of exosomes was determined by using BCA protein assay kit (Pierce). Subsequently, exosome pellets were resuspended in sterile PBS (5 μg/μL).

2.4. Isolation of Kupffer cells (KCs)

Mouse non-parenchymal liver cell population was isolated as previously described [16]. In brief, the liver was sequentially perfused with two solutions. Solution A was composed of the original solution (136 mM NaCl, 5.3 mM KCl, 0.5 mM NaH_2PO_4, 0.4 mM Na_2HPO_4, 9.1 mM HEPES, and 4.1 mM $NaHCO_3$), 0.5 mM EGTA, and 5 mM D-glucose. Solution B was composed of the original solution, 0.04% collagenase IV (Thermo Fisher), and 5 mM $CaCl_2$. After perfusion, livers were excised and shaken in RPMI 1640 with 0.08% type IV collagenase for 15 min. Perfused liver tissue was gently dispersed in an RPMI 1640 medium containing 2% FBS and centrifuged at 50 ×*g* for 3 min at 4 °C to remove parenchymal cells. For KC isolation, the supernatant was washed twice at 500 ×*g* for 8 min. The collected pellet was resuspended in 30% Percoll, and then layered on a 60% Percoll and centrifuged at 800 ×*g* for 20 min. The interface enriched with KCs was aspirated and washed twice with DMEM. For *in vitro* cell stimulation, the collected cells were seeded into plates. After 30 min, the unattached cells were removed, and the remaining attached cells were primary KCs.

2.5. Incubation of macrophage with AMSC-Exo

To determine the effects of AMSC-Exo on macrophage inflammatory response, we added AMSC-Exo, AMSC-Exo$^{miR\text{-}17\text{-}KD}$, or AMSC-Exo$^{miR\text{-}ctrl}$ to cultured RAW264.7 or primary KCs. One hour later, LPS (100 ng/mL) was added to these cultures for 12 h, and then the supernatants were collected for cytokine measurements by using ELISA. Intracellular TXNIP, NLRP3, pro-Casp1, cleaved-Casp1, IL-18, and IL-1β expression levels were measured by Western blot analysis.

2.6. SiRNA and plasmid transfection

SiRNA against TXNIP and scrambled siRNA were purchased from RiboBio and TXNIP overexpression plasmid and control plasmid were constructed by GeneChem. To determine the role of TXNIP in inflammasome activation in macrophages, its siRNA and plasmid were transfected into RAW264.7 cells by using Lipofectamine® 3000 (Thermo Fisher) according to the manufacturer's instructions. At 24 h after transfection, the effects of gene silencing and overexpression were measured by Western blot analysis. Inflammasome activation in these cells by LPS treatment was then evaluated by Western blot analysis and ELISA.

2.7. Isolation and detection of miRNA

Total RNA enriched with miRNAs was isolated from AMSC-Exo or AMSC-Exo-treated cells by using a miRVana miRNA isolation kit (Thermo Fisher) according to the manufacturer's instructions. Complementary DNA was synthesized from the isolated miRNAs by using TaqMan™ mmu-miR-17-specific primers (Thermo Fisher) and TaqMan™ MicroRNA Reverse Transcription Kit (Thermo Fisher). Real-time PCR was then performed following the manufacturer's instructions (Thermo Fisher) to examine miR-17 expression. Data were normalized over the average cycle threshold (CT) value of U6, and the $2^{-\Delta\Delta CT}$ method was used to determine the relative miRNA expression.

2.8. ALF mouse model and AMSC-Exo treatment

Mice (C57BL/6J, aged 5–6 weeks) were intraperitoneally injected with LPS (10 μg/kg, Sigma-Aldrich, St Louis, MO, USA) and D-GalN (400 mg/kg, Sigma-Aldrich) to establish a mouse model of LPS/GalN-induced ALF. AMSC-Exo, AMSC-Exo$^{miR\text{-}17\text{-}KD}$, and AMSC-Exo$^{miR\text{-}ctrl}$ (400 μg total protein in 300 μL volume) ($n = 6$) were administered *via* the tail vein immediately after LPS/GalN injection. In another model of TNF-α/GalN-induced ALF, C57BL/6J mice were intraperitoneally injected with murine recombinant TNF-α (20 μg/kg, Peprotech Inc., Rocky Hill, NJ, USA) and D-GalN (400 mg/kg). AMSC-Exo (400 μg total protein in 300 μL volume) (n = 6) were administered *via* the tail vein immediately after TNF-α/GalN injection. The control group was administered with vehicle alone (n = 6). At 6 h after LPS/GalN or TNF-α/GalN injection, the mice were sacrificed, and serum and liver samples were collected for assessing the extent of liver injury. Serum was evaluated for biochemical parameters. The liver samples were evaluated for histochemistry and Western blot analysis.

2.9. Liver histological and serum biochemical analysis

Liver tissues were processed for paraffin embedding and were sectioned into 4 μm sections. The sections were then routinely stained with hematoxylin and eosin (H&E staining). The serum levels of alanine aminotransferase aspartate (ALT) and aspartate aminotransferase (AST) were measured by using FUJI DRI-CHEM Slide GFP/ALT-PIII and GOT/AST-PIII, respectively, according to the manufacturer's instructions with DRI-CHEM 4000ie (FUJIFILM).

2.10. Cytokine detection by ELISA

The levels of the following cytokines in supernatants from cell cultures or serum were assayed by commercial ELISA kits following the manufacturer's instructions: TNF-α, IFN-γ, IL-1β, IL-6, and IL-18 (MultiSciences, Shanghai, China).

2.11. Western blot analysis

To determine protein expression levels, whole-cell or tissue extracts were lysed with RIPA peptide lysis buffer (Beyotime Biotechnology, Jiangsu, China) containing 1% protease inhibitors (Pierce) and Western blot analysis were performed according to standard procedures. Primary antibodies were used as follows: TXNIP (1:2000, Abcam), NLRP3 (1:1000, Cell Signaling Technology), ASC (1:1000, Abcam), pro-Caspase-1 (1:1000, Abcam), cleaved-Caspase-1 (1:1000, Abcam), IL-1β (1:1000, Abcam), IL-18 (1:1000, Abcam), and GAPDH (1:3000, HuaBio). Protein bands were developed using the enhanced chemiluminescence (ECL) system and were visualized using the ChemiScope Western Blot Imaging System (Clinx Science Instruments Co., Ltd). The gray value assay was performed by using Image J software (Rawak Software, Inc. Germany).

2.12. AMSC-Exo labeling

AMSC-Exo were labeled with a PKH26 Red Fluorescent dye (Sigma-Aldrich), at a dilution of 1:200, according to the manufacturer's instructions. Then the red dye-labeled exosomes were injected into mice *via* tail vein and PBS was used as controls; 6–8 h later, the animals were sacrificed and liver tissues were isolated. The liver sample was then embedded in Tissue-Tek™ CRYO-OCT (Fisher Scientific) and processed for 5 μm sections. The KCs in these sections were stained using a green dye Alexa Fluor 488-labeled CD68 (Abcam). Hepatic distribution of the

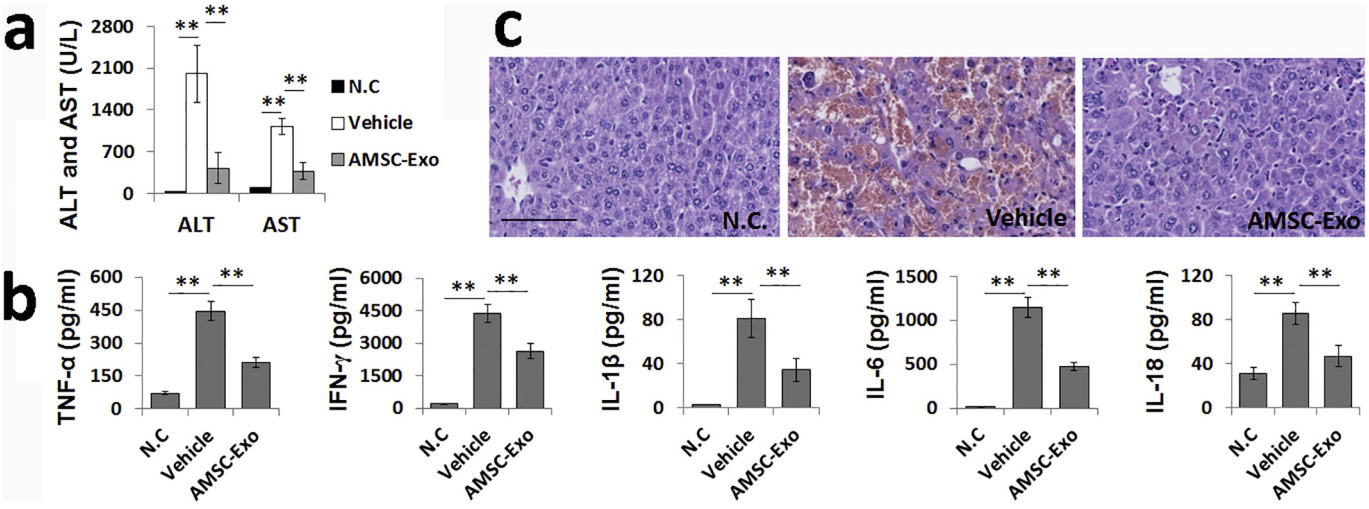

Fig. 2. AMSC-Exo administration ameliorates LPS/D-GalN-induced liver failure. (a and b) Serum levels of ALT, AST, and inflammatory cytokines were elevated by LPS/D-GalN injection (Vehicle group) and significantly decreased by treatment with AMSC-Exo. Data are presented as mean ± SD (Statistical analysis was performed by Student's *t*-test, $^{**}p < .01$, n = 6). (c) Pathological changes in the liver tissue were shown using H&E staining. Scale bar: 100 μm. N.C., normal control.

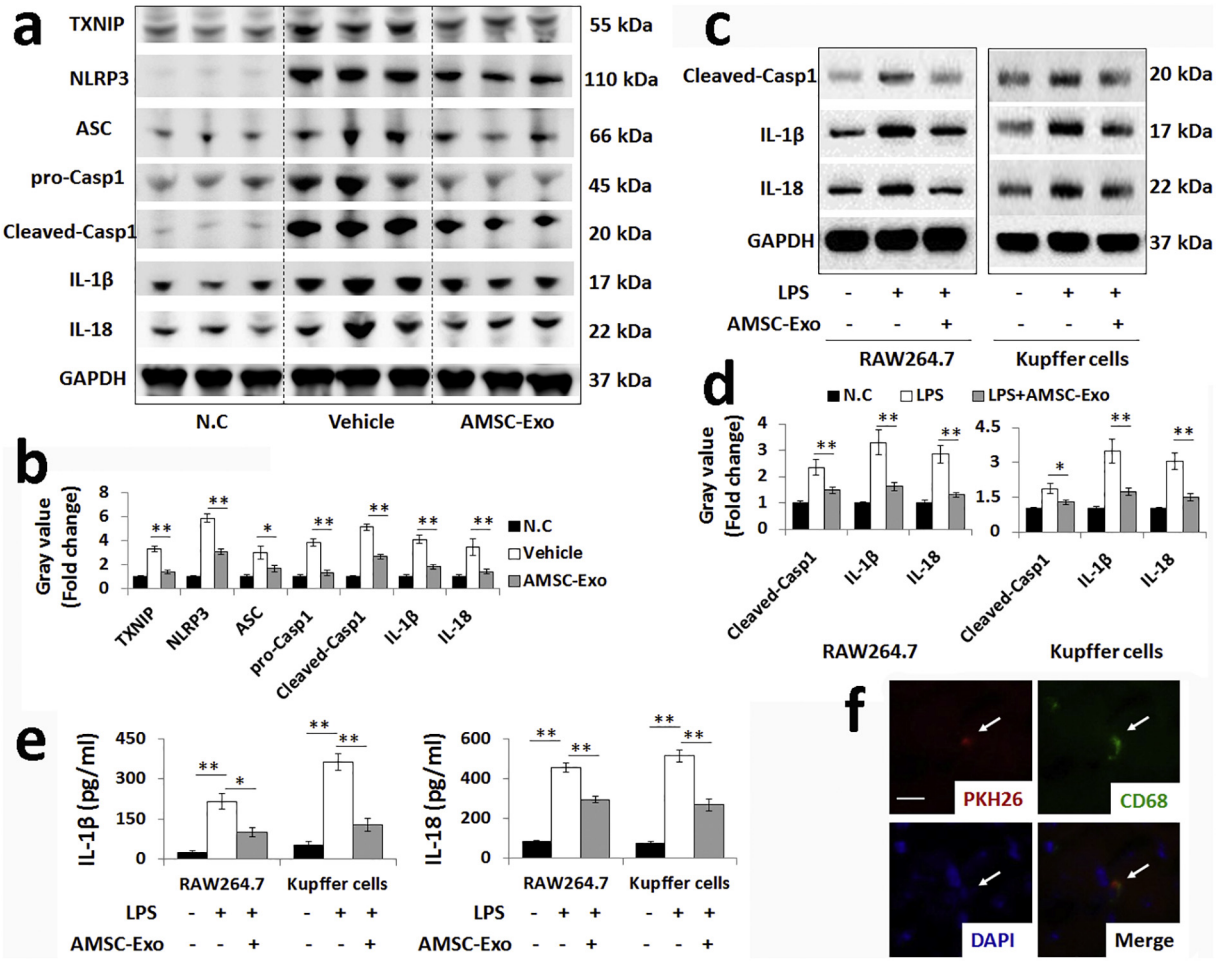

Fig. 3. AMSC-Exo reduce NLRP3 inflammasome activation in macrophages. (a–d) Western blot analysis and gray value assay on expression levels of inflammasome-associated protein in murine liver samples (a and b, n = 6, 3 from 6 samples were shown in a) and macrophages (c and d, n = 3). (e) IL-1β and IL-18 secretion levels from macrophages by LPS exposure were measured by ELISA. (f) PKH26-labeled AMSC-Exo were colocalized with CD68-positive Kupffer cells. Scale bar: 30 μm. Data are presented as mean ± SD (Statistical analysis was performed by Student's *t*-test, $^{*}p < .05$, $^{**}p < .01$). N.C., normal control.

PKH26-labeled AMSC-Exo and their colocalization with KCs were imaged *via* confocal microscopy (Olympus, Center Valley, PA, USA).

2.13. Statistical analysis

Differences between groups were analyzed using conventional Student's *t*-test or ANOVA. Each experiment was repeated at least three times, and the data are presented as mean ± SD. Statistical significance was considered at $P < .05$.

3. Results

3.1. Identification of AMSCs and AMSC-Exo

AMSCs presented a homogeneous population of spindle fibroblast-like cells. They positively expressed CD29, CD44, CD73, CD90.2, and CD105 and negatively expressed CD31, CD45, and I-A/I-E (Fig. 1a). Positive staining of Oil red O or Alcian Blue was observed after adipogenic induction of AMSCs for 14 days (Fig. 1b) or chondrogenic induction for 28 days, respectively (Fig. 1c).

Exosomes were isolated from AMSC culture supernatant. By transmission electron microscopy, we found AMSC-Exo as 40–100 nm microvesicles (Fig. 1d). Western blot analysis also showed that they expressed exosomal markers, such as CD63 and CD81 (Fig. 1e).

3.2. LPS/D-GalN-induced fulminant hepatitis is ameliorated by administration of AMSC-Exo

Next, we determined the therapeutic efficacy of AMSC-Exo in LPS/D-GalN-induced ALF mouse model. The elevation of serum ALT and AST levels (Fig. 2a) and elevated serum inflammatory cytokine concentrations, such as TNF-α, IFN-γ, IL-1β, IL-6, and IL-18 (Fig. 2b), in LPS/D-GalN-injected mice were significantly reduced by AMSC-Exo treatment ($n = 6$) compared with vehicle-treated mice (n = 6) at 6 h after LPS/D-

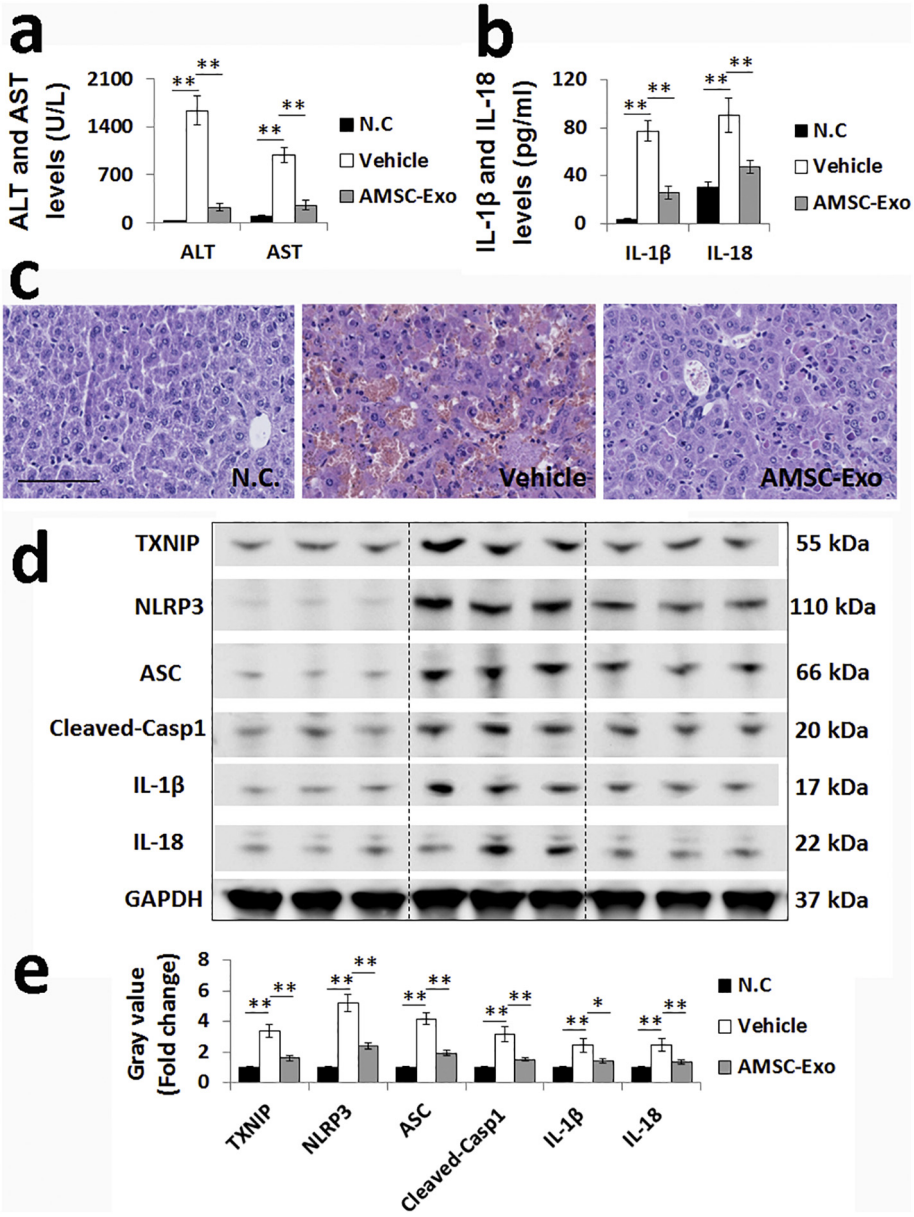

Fig. 4. AMSC-Exo administration ameliorates TNF-α/GalN-induced ALF by inhibiting hepatic inflammasome activation. (a) Serum ALT and AST levels were elevated by TNF-α/GalN injection (Vehicle group) and significantly decreased by treatment with AMSC-Exo. (b) Serum levels of IL-1β and IL-18 were measured by ELISA. (c) Pathological changes in the liver tissue were shown using H&E staining. Scale bar: 100 μm. (d and e) Western blot analysis (d) and gray value assay (e) on the expression levels of inflammasome-associated proteins in murine liver samples. Data are presented as mean ± SD (Statistical analysis was performed by Student's *t*-test, *p < .05, **p < .01, n = 6). N.C., normal control.

GalN injection. Histopathological analysis also showed an almost normal appearance with no necrosis in the liver of AMSC-Exo administration group (Fig. 2c), indicating that LPS/D-GalN-induced hepatitis was markedly ameliorated by AMSC-Exo treatment.

3.3. AMSC-Exo treatment reduces NLRP3 inflammasome activation in macrophages

The activation of NLRP3 inflammasome plays an important role in ALF [7]. Therefore, we investigated whether AMSC-Exo-based therapy has an effect on NLRP3 inflammasome activation. As shown in Fig. 3a and b, the upregulated protein expressions of TXNIP, NLRP3, ASC, pro-Casp1, cleaved-Casp1, IL-18, and IL-1β in the liver by LPS/D-GalN exposure were significantly decreased in AMSC-Exo-treated group compared with those in the vehicle-treated group. The reduced activation of hepatic inflammasome was consistent with the decreased serum levels of IL-1β and IL-18 as mentioned above (Fig. 2b).

The effect of AMSC-Exo on inflammasome inhibition was also confirmed in another model of ALF. As shown in Fig. 4, AMSC-Exo administration could ameliorate GalN/TNF-α-induced ALF through downregulating the expression levels of inflammasome-related genes in murine liver tissue.

As NLRP3 inflammasome is reported to mainly be expressed in macrophages [17,18], we further investigated the effects of AMSC-Exo on

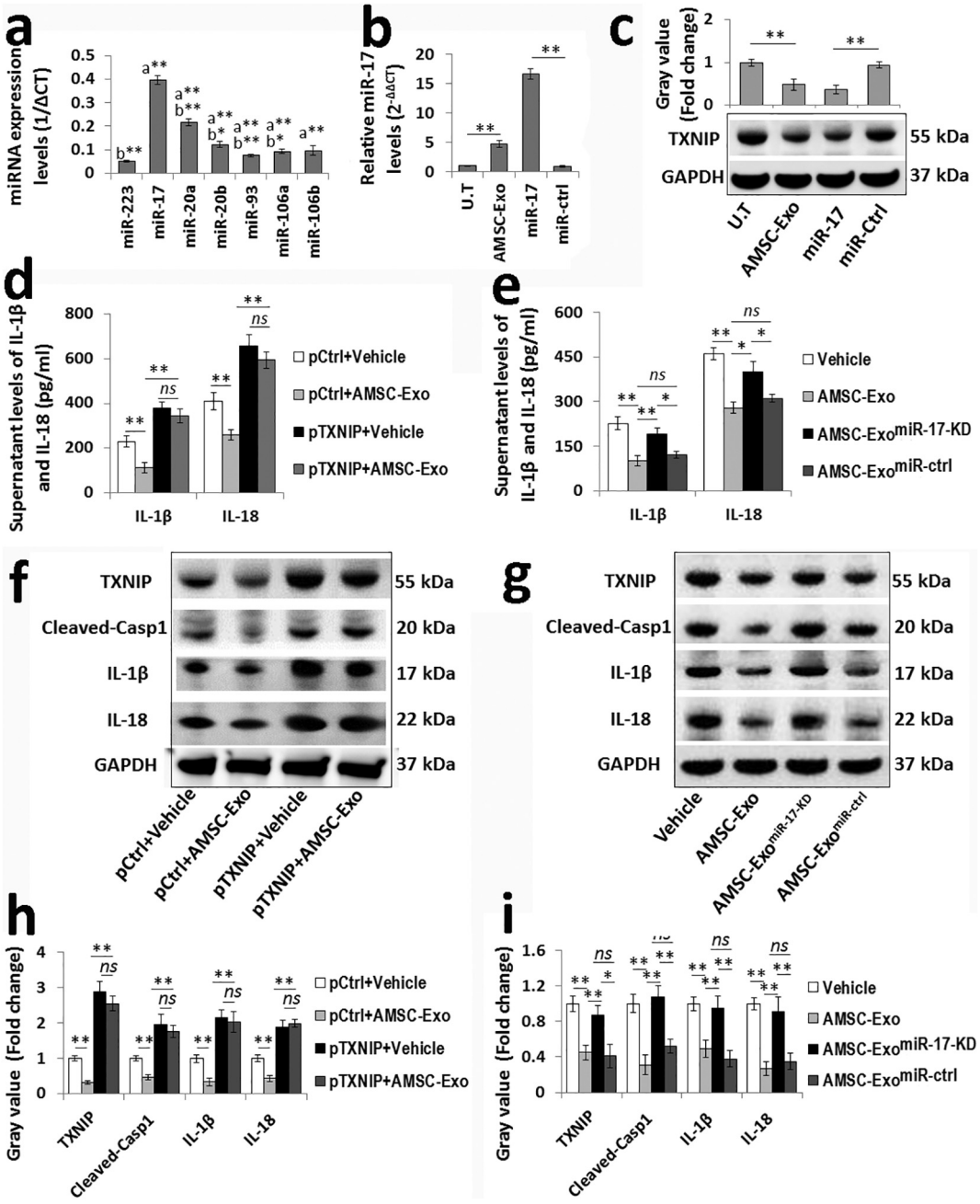

Fig. 5. AMSC-Exo suppress inflammasome activation by miR-17-mediated TXNIP inhibition. (a) qPCR detection of miR-223 and miR-17 family miRNAs (miR-17, miR-20a/b, miR-93, miR-106a/b) relative expression levels in AMSC-Exo (a, compared with miR-223; b, compared with miR-17). (b and c) qPCR detection of miR-17 (b) and Western blot analysis of TXNIP (c) expression levels in RAW264.7 cells treated with AMSC-Exo or transfected with miR-17 or control miRNA (miR-ctrl). U.T, untreated. (d and e) IL-1β and IL-18 secretion levels of LPS-stimulated RAW264.7 cells were measured by ELISA (*ns*, nonsense). (f–i) Protein levels of TXNIP, cleaved-Casp1, IL-1β, and IL-18 in LPS-stimulated RAW264.7 cells were measured by Western blot analysis (f and g) and then quantified by gray value assay (h and i). Data are presented as mean ± SD (Statistical analysis was performed by Student's *t*-test, $^{*}p < .05$, $^{**}p < .01$, $n = 3$). pCtrl, transfection with a control vector; pTXNIP, transfection with a TXNIP overexpression plasmid; AMSC-Exo$^{miR\text{-}17\text{-}KD}$, miR-17-knock down AMSC-Exo.

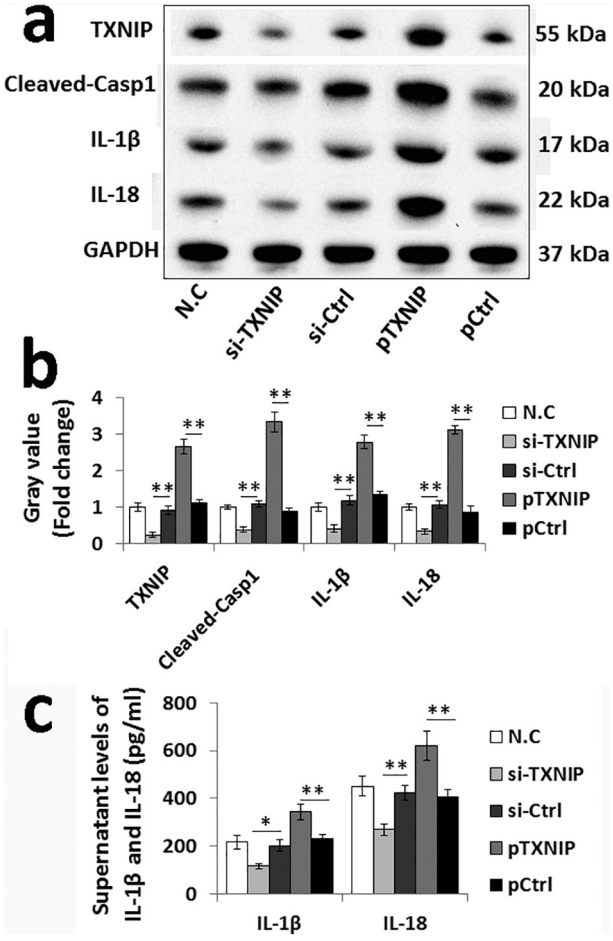

Fig. 6. Change of TXNIP expression affects NLRP3 inflammasome activation in macrophages. (a and b) Western blot analysis (a) and gray value assay (b) on expression levels of TXNIP, cleaved-Casp1, IL-1β, and IL-18 in LPS-stimulated RAW264.7 cells transfected by TXNIP siRNA (si-TXNIP), overexpression plasmid (pTXNIP), or corresponding controls (si-Ctrl and pCtrl). (c) IL-1β and IL-18 secretion levels of these cells were measured by ELISA. Data are presented as mean ± SD (Statistical analysis was performed by Student's *t*-test, $^{*}p < .05$, $^{**}p < .01$, n = 3).

inflammasome activation by adding AMSC-Exo to LPS-primed mouse macrophage cell line, RAW264.7, or primary hepatic macrophage, KCs. As shown in Fig. 3c and d, the NLRP3 inflammasome activation, indicated by cleaved-Casp1, IL-1β, and IL-18 expression, was markedly suppressed in macrophages by AMSC-Exo treatment as assessed by Western blot analysis. Also, the IL-1β and IL-18 secretion from macrophages was reduced by AMSC-Exo treatment (Fig. 3e). Moreover, the red dye PHK26-labeled AMSC-Exo was shown to be colocalized with CD68-positive KCs by *i.v.* injection, further suggesting that AMSC-Exo can target macrophages and then modulate their function (Fig. 3f).

Together, these data indicate that AMSC-Exo alleviates LPS/GalN-induced hepatitis by inhibiting NLRP3 inflammasome activation in macrophages.

3.4. MiR-17-containing AMSC-Exo reduce inflammasome activation by targeting TXNIP

Our previous studies showed that AMSC-Exo exhibit a therapeutic efficacy by mediating miRNA transmission [5,19]. As the miR-223 and miR-17 family, including miR-17 and miR-20a, have been reported to target NLRP3 and TXNIP [20–22], respectively, we then analyzed the expressions of these miRNAs in AMSC-Exo. In contrast to the low level of miR-223, AMSC-Exo contained high levels of miR-17 family miRNAs, especially miR-17 (Fig. 5a). Further study showed that by incubating with AMSC-Exo, the TXNIP expression was downregulated corresponding to the increased miR-17 level in RAW264.7 cells as those by miR-17 transfection (Fig. 5b and c), indicating that miR-17-mediated TXNIP inhibition may participate in the therapeutic mechanism of AMSC-Exo treatment.

TXNIP is known as a key player in the activation of NLRP3-inflammasome and we also confirmed that the changes of TXNIP expression could affect NLRP3 inflammasome activation in macrophages (Fig. 6). To determine whether AMSC-Exo suppresses inflammasome activation by decreasing TXNIP level, we transduced either a control vector or a TXNIP overexpression plasmid into RAW264.7 cells combined with AMSC-Exo treatment. We found that the restoration of TXNIP reversed the inhibitory effects of AMSC-Exo on inflammasome activation in LPS-primed RAW264.7 cells (Fig. 5d, f and h). To further confirm whether the inhibitory effect of AMSC-Exo on inflammasome activation is caused by miR-17, AMSCs were transfected with miR-17 inhibitor or scrambled-miRNA inhibitor for producing the miR-17-knock down AMSC-Exo, AMSC-Exo$^{miR\text{-}17\text{-}KD}$, and the control exosomes, AMSC-Exo$^{miR\text{-}ctrl}$, respectively. As we expected, AMSC-Exo$^{miR\text{-}17\text{-}KD}$ could not effectively suppress the inflammasome activation in LPS-primed RAW264.7 cells as determined by the expressions of TXNIP, cleaved-Casp1, IL-1β, and IL-18 and the secretions of IL-1β and IL-18. However, the inhibition effect of AMSC-Exo$^{miR\text{-}ctrl}$ treatment on inflammasome activation was equivalent to that of naïve AMSC-Exo treatment (Fig. 5e, g and i).

Subsequent *in vivo* study also confirmed the above results as the therapeutic effects of AMSC-Exo on ALF were partly abolished by introducing miR-17 inhibitor. As shown in Fig. 7a–c, the pathologic alteration and the upregulated serum ALT, AST, and inflammatory cytokines induced by LPS/D-GalN could not be effectively attenuated by AMSC-Exo$^{miR\text{-}17\text{-}KD}$ administration. In addition, the upregulated hepatic expression levels of TXNIP, NLRP3, ASC, cleaved-Casp1, IL-1β and IL-18 were not reduced obviously in the AMSC-Exo$^{miR\text{-}17\text{-}KD}$ administration group as compared to those in the AMSC-Exo$^{miR\text{-}ctrl}$ administration group (Fig. 7d and e). These data suggest that miR-17-mediated TXNIP inhibition is partly involved in the reduction of NLRP3 inflammasome activation in macrophages by AMSC-Exo treatment.

4. Discussion

MSC derived exosomes have yielded beneficial effects in several experimental models of organ injury [23,24]. Recently, the therapeutic effects of exosomes from bone marrow-, chorionic plate-, umbilical cord-, or induced pluripotent stem cell-derived MSCs have been reported in a variety of animal models of liver disease, including concanavalin A or acetaminophen-induced acute liver injury, CCl_4-induced liver fibrosis, liver antigen S100-induced autoimmune hepatitis, or I/R-induced hepatic injury [25–30]. Our previous studies also showed that the exosomes produced by miR-122-modified AMSCs can alleviate liver fibrosis and enhance hepatocellular carcinoma chemosensitivity *via* exosome-mediated miR-122 delivery [5,19]. Thus administration of MSC-derived exosomes may represent as an ideal cell-free therapy for liver diseases. In this study we investigated the effects and underlying mechanisms of AMSC-Exo on LPS/D-GalN-induced ALF. We found that AMSC-Exo exerted protective effects against ALF by reducing NLRP3 inflammasome activation in macrophages through miR-17-mediated TXNIP inhibition.

Inflammasome activation has been studied in human and experimental ALF and has been identified as a major contributor to hepatocyte damage and immune cell activation and amplification in fulminant hepatitis [7]. Its activation uniquely occurs in two steps. The first step is the activation of TLRs by different molecules DAMPs and PAMPs. TLRs are expressed in a variety of hepatic parenchymal cells and nonparenchymal cells, such as hepatocytes and KCs. TLR activation, in turn, up-regulates the transcriptions of inflammasome-related components, including NLRP3, pro-IL-1β, and pro-IL-18. The second step of

inflammasome activation is the oligomerization of NLRP3 and subsequent assembly of NLRP3, ASC, and procaspase-1 into a complex. This triggers the transformation of procaspase-1 to caspase-1, which leads to the proteolytical maturation and secretion of inflammatory cytokines IL-1β and IL-18 [31]. Our results showed that *i.v.* administration of AMSC-Exo significantly suppressed LPS/GalN- or TNF-α/GalN-induced inflammasome activation, which was determined by the hepatic expression levels of NLRP3, ASC, and cleaved-caspase-1 and the serum levels of IL-1β and IL-18. These results support that the inhibition of hepatic inflammasome activation contributes to the observed therapeutic effects of AMSC-Exo against ALF.

KCs, as a subgroup of macrophages that residents in the liver, play a pivotal role in modulating hepatic immune microenvironment and inflammatory response in ALF [32]. At the onset of ALF, KCs are activated and its TLR4 expression are upregulated by binding with LPS. This activation induces multiple cellular signaling pathways, such as NF-κB, mitogen-activated protein kinase, p38, and c-jun N-terminal kinase, and then triggers the activation of NLRP3 inflammasome to produce a large amount of pro-inflammatory cytokines, such as IL-18 and IL-1β [33]. The imbalance of pro-inflammatory and anti-inflammatory cytokines finally causes the uncontrolled inflammatory action and facilitates the progression of ALF. Thus, the inhibition of abnormal activated macrophages and its inflammasome activation may be an effective strategy for ALF prevention and treatment. Our *in vitro* studies further showed that AMSC-Exo could successfully decrease the upregulated expression

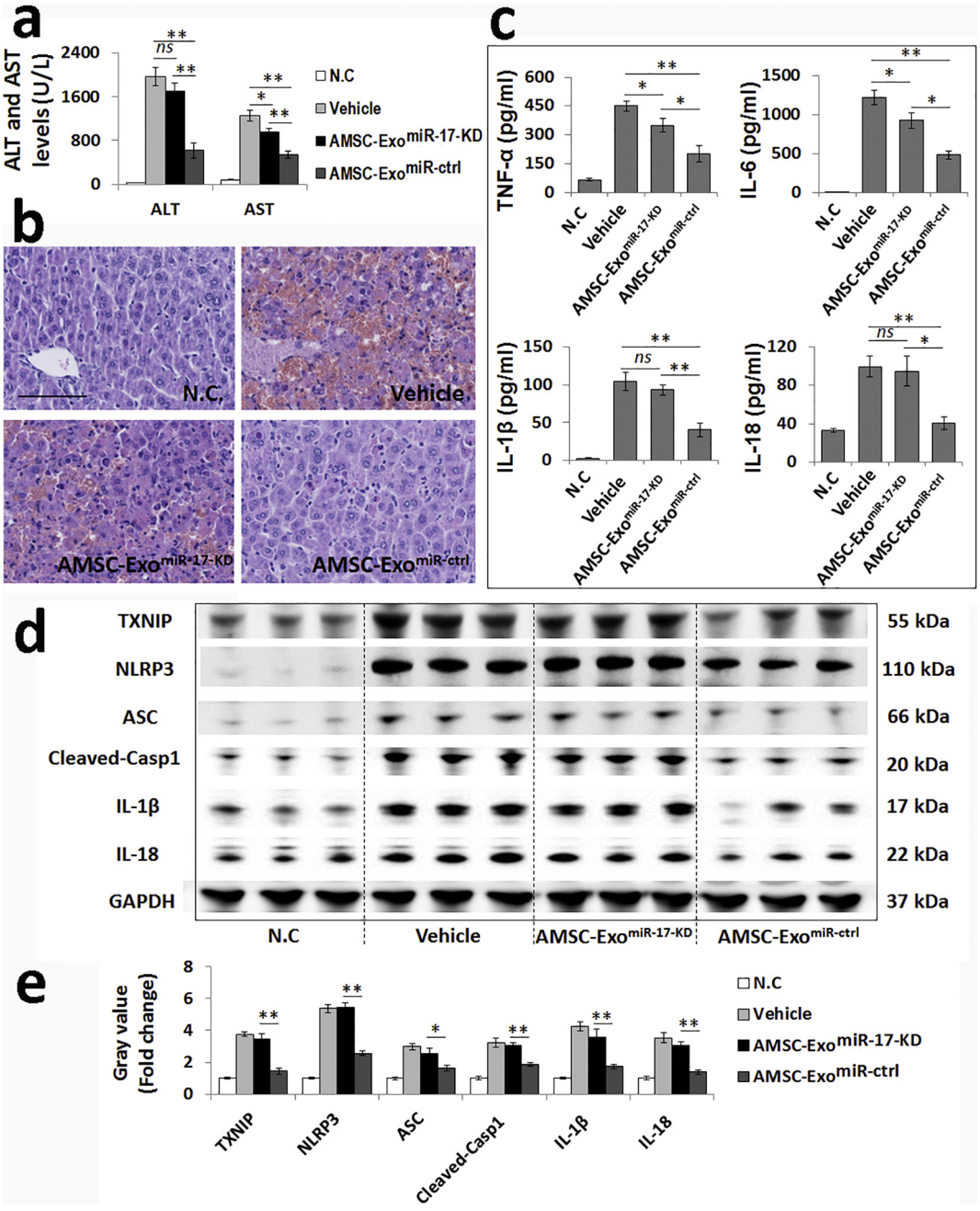

Fig. 7. Therapeutic effects of AMSC-Exo on ALF are partly abolished by introducing miR-17 inhibitor. (a) Inhibitor-mediated miR-17 knock-down weakened AMSC-Exo (AMSC-Exo$^{miR\text{-}17\text{-}KD}$) efficacy in decreasing serum ALT and AST levels compared with AMSC-Exo$^{miR\text{-}ctrl}$. (b) Pathological changes in the liver tissue were shown by H&E staining. Scale bar: 100 μm. (c) Serum levels of inflammatory cytokines were measured by ELISA. (d and e) Protein levels of TXNIP, NLRP3, ASC, cleaved-Casp1, IL-1β, and IL-18 in murine liver samples were measured by Western blot analysis (d) and then quantified by gray value assay (e). Data are presented as mean ± SD (Statistical analysis was performed by Student's *t*-test, $^{*}p < .05$, $^{**}p < .01$, *ns*: nonsense, $n = 6$, 3 from 6 samples were shown in d). N.C., normal control.

levels of NLRP3, cleaved-Casp1, IL-1β, and IL-18 in Raw264.7 cells and primary KCs and reduce the IL-1β and IL-18 secretion from these macrophages by LPS-exposure. These *in vitro* data combined with the observed effects of AMSC-Exo *in vivo* suggest that AMSC-Exo can be used as a potential therapeutic strategy for ALF by inhibiting NLRP3 inflammasome activation in macrophages. The colocalization of PHK26-labeled AMSC-Exo with CD68-positive KCs by *i.v.* administration further supported that the protection of AMSC-Exo against ALF is associated with exosome-mediated functional regulation of macrophage.

It is well known that exosome can act as an intercellular communication vehicle by delivering its contents between cells for modulating or mediating cellular processes [34]. Similar to exosomes in general, MSC-derived exosomes carry complex cargo, including nucleic acids, proteins, and lipids. Through microarray analysis, >150 miRNAs have been identified in the cargo of MSC-derived exosomes and it is various among the MSCs from different sources [35,36]. Chorionic plate-derived MSCs were shown to promote liver regeneration through miR-125b-mediated regulation of Hh signaling and bone marrow-derived MSCs were shown to increase myocardial contractility through exosomal miR-223-mediated modulation of calcium handling gene expression [27,37]. Thus, we speculated that the inhibitory action of AMSC-Exo on inflammasome activation may also due to exosome-mediated miRNA shuttling. MiR-223 is the most widely reported miRNA that regulates inflammasome activation by targeting the 3′-UTR of NLRP3 mRNA. It was shown that miR-223 is highly expressed in BMSC-derived exosomes, and miR-223-containing exosomes can protect against experimental autoimmune hepatitis *via* miR-223-mediated downregulation of NLRP3 in hepatocytes [29]. However, miR-223 is almost undetectable in AMSC-Exo, which may be related to its expression mainly confined to myeloid cells, whereas AMSC-Exo containes high levels of miR-17 family miRNAs, especially miR-17. As miR-17 has been reported to target TXNIP [21], which plays an essential role in the activation of the NLRP3-inflammasome [10,38], we hypothesized that the inhibitory effect of AMSC-Exo on inflammasome activation may be caused by exosome-mediated miR-17 shuttling. The subsequent result of miR-17 upregulation in macrophages by incubation with AMSC-Exo supported this speculation. Moreover, the therapeutic effects of the exosomes derived from miR-17 inhibitor-transfected AMSCs on ALF were partly abolished, and AMSC-Exo$^{miR\text{-}17\text{-}KD}$ could not effectively suppress TXNIP expression and consequent inflammasome activation *in vitro* and *in vivo* compared with AMSC-Exo$^{miR\text{-}ctrl}$. This finding further indicates that the reduction of NLRP3 inflammasome activation by AMSC-Exo treatment is partly dependent on miR-17-mediated TXNIP inhibition.

In conclusion, the present study showed that AMSC-Exo can ameliorate LPS/GalN-induced ALF by reducing NLRP3 inflammasome activation in macrophages. Exosome-mediated miR-17 shuttling is involved in the therapeutic effects of AMSC-Exo against ALF by targeting TXNIP and consequent NLRP3 inflammasome blockage. This study provides novel insights into MSC-Exo-based therapy and its potential mechanism. Administration of AMSC-Exo may present as a novel therapeutic strategy for preventing fulminant hepatitis, as well as other TXNIP/NLRP3 inflammasome-related inflammatory liver diseases.

Funding sources

This work was supported by the Key R & D Projects of Zhejiang Province (Grant No. 2018C03019) and the National Natural Science Fund (Grant No. 81470851 and 81500616).

Conflict of interest statement

The authors declare that they have no competing interests.

Author contributions

Y.N.L. conceived of the study and participated in its coordination and writing. G.H.L. performed the *in vivo* experiment and drafted the manuscript. A.C.L. and T.B.Z. performed the *in vitro* experiments. J.J.Q. and D. Y. performed the data analysis and interpretation. M. Z. and Z. C. participated in study design and coordination. All authors read and approved the final manuscript.

References

[1] Patel P, Okoronkwo N, Pyrsopoulos NT. Future approaches and therapeutic modalities for acute liver failure. Clin Liver Dis 2018;22(2):419–27.
[2] Volarevic V, Nurkovic J, Arsenijevic N, Stojkovic M. Concise review: therapeutic potential of mesenchymal stem cells for the treatment of acute liver failure and cirrhosis. Stem Cells 2014;32(11):2818–23.
[3] Lou G, Chen Z, Zheng M, Liu Y. Mesenchymal stem cell-derived exosomes as a new therapeutic strategy for liver diseases. Exp Mol Med 2017;49(6):e346.
[4] Phinney DG, Pittenger MF. Concise review: MSC-derived exosomes for cell-free therapy. Stem Cells 2017;35(4):851–8.
[5] Lou G, Yang Y, Liu F, Ye B, Chen Z, Zheng M, et al. MiR-122 modification enhances the therapeutic efficacy of adipose tissue-derived mesenchymal stem cells against liver fibrosis. J Cell Mol Med 2017;21(11):2963–73.
[6] Schroder K, Tschopp J. The inflammasomes. Cell 2010;140(6):821–32.
[7] Woolbright BL, Jaeschke H. Role of the inflammasome in acetaminophen-induced liver injury and acute liver failure. J Hepatol 2017;66(4):836–48.
[8] He Y, Hara H, Núñez G. Mechanism and regulation of NLRP3 inflammasome activation. Trends Biochem Sci 2016;41(12):1012–21.
[9] Zhou R, Tardivel A, Thorens B, Choi I, Tschopp J. Thioredoxin-interacting protein links oxidative stress to inflammasome activation. Nat Immunol 2010;11:136–40.
[10] Cao Z, Fang Y, Lu Y, Tan D, Du C, Li Y, et al. Melatonin alleviates cadmium-induced liver injury by inhibiting the TXNIP-NLRP3 inflammasome. J Pineal Res 2017;62(3).
[11] Liu X, Wang T, Liu X, Cai L, Qi J, Zhang P, et al. Biochanin A protects lipopolysaccharide/D-galactosamine-induced acute liver injury in mice by activating the Nrf2 pathway and inhibiting NLRP3 inflammasome activation. Int Immunopharmacol 2016;38:324–31.
[12] Shin TH, Kim HS, Kang TW, Lee BC, Lee HY, Kim YJ, et al. Human umbilical cord blood-stem cells direct macrophage polarization and block inflammasome activation to alleviate rheumatoid arthritis. Cell Death Dis 2016;7(12):e2524.
[13] Miteva K, Pappritz K, Sosnowski M, El-Shafeey M, Müller I, Dong F, et al. Mesenchymal stromal cells inhibit NLRP3 inflammasome activation in a model of Coxsackievirus B3-induced inflammatory cardiomyopathy. Sci Rep 2018;8(1):2820.
[14] Yuan X, Wang X, Chen C, Zhou J, Han M. Bone mesenchymal stem cells ameliorate ischemia/reperfusion-induced damage in renal epithelial cells via microRNA-223. Stem Cell Res Ther 2017;8(1):146.
[15] Wang T, Wang Z, Yang P, Xia L, Zhou M, Wang S, et al. PER1 prevents excessive innate immune response during endotoxin-induced liver injury through regulation of macrophage recruitment in mice. Cell Death Dis 2016;7:e2176.
[16] Yu X, Lan P, Hou X, Han Q, Lu N, Li T, et al. HBV inhibits LPS-induced NLRP3 inflammasome activation and IL-1β production via suppressing the NF-κB pathway and ROS production. J Hepatol 2017;66(4):693–702.
[17] Pourcet B, Zecchin M, Ferri L, Beauchamp J, Sitaula S, Billon C, et al. Nuclear receptor subfamily 1 group D member 1 regulates circadian activity of NLRP3 inflammasome to reduce the severity of fulminant hepatitis in mice. Gastroenterology 2018;154(5):1449–64.
[18] Alvarado R, To J, Lund ME, Pinar A, Mansell A, Robinson MW, et al. The immune modulatory peptide FhHDM-1 secreted by the helminth Fasciola hepatica prevents NLRP3 inflammasome activation by inhibiting endolysosomal acidification in macrophages. FASEB J 2017;31(1):85–95.
[19] Lou G, Song X, Yang F, Wu S, Wang J, Chen Z, et al. Exosomes derived from miR-122-modified adipose tissue-derived MSCs increase chemosensitivity of hepatocellular carcinoma. J Hematol Oncol 2015;8:122.
[20] Bauernfeind F, Rieger A, Schildberg FA, Knolle PA, Schmid-Burgk JL, Hornung V. NLRP3 inflammasome activity is negatively controlled by miR-223. J Immunol 2012;189(8):4175–81.
[21] Dong D, Fu N, Yang P. MiR-17 downregulation by high glucose stabilizes thioredoxin-interacting protein and removes thioredoxin inhibition on ASK1 leading to apoptosis. Toxicol Sci 2016;150(1):84–96.
[22] Chen M, Li W, Zhang Y, Yang J. MicroRNA-20a protects human aortic endothelial cells from Ox-LDL-induced inflammation through targeting TLR4 and TXNIP signaling. Biomed Pharmacother 2018;103:191–7.
[23] Keshtkar S, Azarpira N, Ghahremani MH. Mesenchymal stem cell-derived extracellular vesicles: novel frontiers in regenerative medicine. Stem Cell Res Ther 2018;9(1):63.
[24] Luther KM, Haar L, McGuinness M, Wang Y, Lynch Iv TL, Phan A, et al. Exosomal miR-21a-5p mediates cardioprotection by mesenchymal stem cells. J Mol Cell Cardiol 2018;119:125–37.
[25] Tamura R, Uemoto S, Tabata Y. Immunosuppressive effect of mesenchymal stem cell-derived exosomes on a concanavalin A-induced liver injury model. Inflamm Regen 2016;36:26.
[26] Tan CY, Lai RC, Wong W, Dan YY, Lim SK, Ho HK. Mesenchymal stem cell-derived exosomes promote hepatic regeneration in drug-induced liver injury models. Stem Cell Res Ther 2014;5(3):76.

[27] Hyun J, Wang S, Kim J, Kim GJ, Jung Y. MicroRNA125b-mediated Hedgehog signaling influences liver regeneration by chorionic plate-derived mesenchymal stem cells. Sci Rep 2015;5:14135.
[28] Li T, Yan Y, Wang B, Qian H, Zhang X, Shen L, et al. Exosomes derived from human umbilical cord mesenchymal stem cells alleviate liver fibrosis. Stem Cells Dev 2013;22(6):845–54.
[29] Chen L, Lu FB, Chen DZ, Wu JL, Hu ED, Xu LM, et al. BMSCs-derived miR-223-containing exosomes contribute to liver protection in experimental autoimmune hepatitis. Mol Immunol 2018;93:38–46.
[30] Du Y, Li D, Han C, Wu H, Xu L, Zhang M, et al. Exosomes from human-induced pluripotent stem cell-derived mesenchymal stromal cells (hiPSC-MSCs) protect liver against hepatic ischemia/reperfusion injury via activating sphingosine kinase and sphingosine-1-phosphate signaling pathway. Cell Physiol Biochem 2017;43(2):611–25.
[31] Negash AA, Gale Jr M. Hepatitis regulation by the inflammasome signaling pathway. Immunol Rev 2015;265(1):143–55.
[32] Ju C, Tacke F. Hepatic macrophages in homeostasis and liver diseases: from pathogenesis to novel therapeutic strategies. Cell Mol Immunol 2016;13(3):316–27.
[33] Del Campo JA, Gallego P, Grande L. Role of inflammatory response in liver diseases: therapeutic strategies. World J Hepatol 2018;10(1):1–7.
[34] Colombo M, Raposo G, Théry C. Biogenesis, secretion, and intercellular interactions of exosomes and other extracellular vesicles. Annu Rev Cell Dev Biol 2014;30:255–89.
[35] Ferguson SW, Wang J, Lee CJ, Liu M, Neelamegham S, Canty JM, et al. The microRNA regulatory landscape of MSC-derived exosomes: a systems view. Sci Rep 2018;8(1):1419.
[36] Barrera-Ramirez J, Lavoie JR, Maganti HB, Stanford WL, Ito C, Sabloff M, et al. Micro-RNA profiling of exosomes from marrow-derived mesenchymal stromal cells in patients with acute myeloid leukemia: implications in leukemogenesis. Stem Cell Rev 2017;13(6):817–25.
[37] Mayourian J, Ceholski DK, Gorski PA, Mathiyalagan P, Murphy JF, Salazar SI, et al. Exosomal microRNA-21-5p mediates mesenchymal stem cell paracrine effects on human cardiac tissue contractility. Circ Res 2018;122(7):933–44.
[38] Liu Y, Lian K, Zhang L, Wang R, Yi F, Gao C, et al. TXNIP mediates NLRP3 inflammasome activation in cardiac microvascular endothelial cells as a novel mechanism in myocardial ischemia/reperfusion injury. Basic Res Cardiol 2014;109(5):415.